Ultra-low background alpha particle counter using pulse shape analysis

W. K. Warburton, *Member, IEEE, Brendan Dwyer-McNally, Michael Momayezi, and John E. Wahl*

***Abstract*--The need to measure alpha particle emissivities at levels below 0.005 α/cm^2-hr is becoming increasingly important in fundamental physics experiments (e.g. neutrino and rare decay measurements), environmental monitoring, nuclear activities monitoring and semiconductor packaging materials,. Present counters can barely reach this level, being limited both by cosmic ray events and by their own alpha emissions. Here we report a detector capable of measurements at 0.00005 α/cm^2-hr using a large electrode ionization chamber with digital pulse shape analysis to locate the point of emission of each alpha particle. Filled with 1 atm N_2, the counter is essentially blind to both environmental gamma-rays and cosmic ray muon showers, so its background becomes limited by the pulse shape analysis's ability to distinguish different points of alpha particle origin.**

The counter's geometry intentionally exaggerates differences between signals originating from its different surfaces, with an inter-electrode separation D over 3 times the alpha particle range L. Since signal risetimes equal charge drift times, anode events have 8-10 μs risetimes, while sample event risetimes are 30-35 μs and readily distinguished. Integrated charge also increases with drift length, producing a 2 to 1 difference between sample and anode events. Applying both risetime and amplitude cuts distinguishes between sample and anode emitted alpha particles at about 1 part in 1000. A guard electrode surrounding the anode allows alpha particles from the counter's sidewalls to be rejected at a similar ratio, so that essentially only alpha particles emanating from the sample are finally counted.

I. INTRODUCTION

Most materials emit alpha particles, either because they contain trace amounts of radioactive materials or because they have been contaminated by contact with radioactive materials, most commonly radon in the atmosphere. The ability to measure materials' alpha particle emissivity (typically expressed as α/cm^2-hr) therefore becomes important in applications that are sensitive to alpha particles. These include low background fundamental physics experiments (e.g. rare decay and neutrino detection measurements), nuclear activities and environmental monitoring, and semiconductor packaging materials production.

The latter application was the primary driving force behind the present work, since alpha particles can change the logic state of electronic circuits. Industry roadmaps therefore project a coming need for solder materials whose emissivities should be less than 0.0005 α/cm^2-hr, [1] which poses a problem, since current alpha particle counters are limited to about 0.005 α/cm^2-hr by their inherent radioactivity in the case of gas filled proportional counters [2] or to about 0.06 α/cm^2-hr by cosmic ray interactions within their active counting volumes in the case of silicon diode detectors [3].

We report here a novel approach, using pulse shape analysis in an ionization chamber, that produces background levels approaching 0.00005 α/cm^2-hr, about 100 times better than is currently possible. In Sec. II we give the physical basis of the method; in Sec. III we present typical signal traces from the counter; in Sec. IV we describe our pulse shape analysis algorithms and their results; followed by conclusions in Sec. V.

II. THE BASIS OF THE METHOD

A. Description of the apparatus

The counter is essentially a chamber, constructed primarily of 2 cm thick acrylic plastic that is 50 cm square by 15 cm high. Ref. [4] contains complete details. On the upper inside of the box is a central square anode 40 cm on a side whose perimeter is surrounded by a guard electrode 4.5 cm across, with an 0.5 cm gap. Both electrodes are biased to -1,000 V through 18 MΩ resistors and coupled by 10 nF capacitors to two preamplifiers whose outputs are passed to two interconnected digital signal processors that both capture signal traces for analysis whenever either detects a pulse. The counter's internal electric field causes charge tracks generated by alpha particles emitted within the chamber to drift to the anode, guard or both, depending upon their point of emanation within the chamber.

The bottom of the chamber is a removable sample tray that is covered with a grounded electrode. Samples to be measured are placed upon the sample tray, which is then raised to seal the counting chamber. A source of high purity boil-off N_2 gas is connected to the chamber through two remotely controlled valves that allow it to first be purged at 20 l/m and then operated at 5-7 l/m. Purging is required because either oxygen

Manuscript received October 18, 2004.

This work was supported in part by the National Institute of Standards and Technology under SBIR Contract 50-DKNB-1-SB085.

W. K. Warburton, B. Dwyer-McNally, and M. Momayezi are with X-ray Instrumentation Associates, Newark, CA 94560 USA (telephone: 510-494-9020; e-mail: bill@xia.com, brendan@xia.com, and momayezi@xia.com, respectively).

J. E. Wahl was with X-ray Instrumentation Associates, Newark, CA 94560 USA. He is now with the MIT Lincoln Laboratory, Lexington, MA 02420 USA (telephone: 781-981-4234, e-mail: wahl@ll.mit.edu).

or water vapor would trap drifting electrons before they reached the anode. Purging typically takes only 10-15 minutes.

Four field shaping electrodes surround the chamber's exterior sidewalls. Their function is to preserve a uniform electric field within the counter all the way to the sidewalls. Each electrode consists of about 50 traces on a PC board, arranged parallel to its sidewall's bottom edge at 3 mm intervals and interconnected by 200 KΩ resistors, for a 10 MΩ total resistance. These electrodes are grounded at the bottom and biased to the same potential as the anode at the top.

For ideally sized samples, which are at least as large as the anode (1,600 cm area) there are then only three types of surface inside the counter that might emit alpha particle: the sample, the acrylic sidewalls, and the anode/guard electrodes, which are currently made of 50 μm polished stainless steel.

B. Simple charge collection theory

An often unappreciated feature of charge collection is that, per the Shockley-Ramo theorem, [5] a current flows in the external circuit *only* while the charge is moving within the counter's active volume due to the applied potential V and ceases when the charge is "collected" at an electrode. Thus, an external preamplifier integrating this "induced charge" produces a signal whose risetime equals the maximum charge drift time and whose amplitude increases with the distance the moving charge travels within the detector. In our nominally parallel plate geometry, the induced current is the same as the current of the drifting charge q itself,: $i_q = qv_q / R$, where R is the chamber height. The electron's drift velocity v_e in N_2 equals its mobility μ_e times the electric field V/R, so it is straightforward to compute both its drift time and the total induced charge integrated onto the preamplifier's feedback capacitor C_f from its motion. For a uniform charge track of N electrons emanating from the *anode*, charge disappears linearly in time as it is collected, so that the resultant signal $S_a(t)$ is a parabola given by:

$$S_a(t) = \frac{Ne\mu_e V}{C_f R^2}\left(t - \frac{t^2}{2t_a}\right), \qquad (1)$$

whose rise time (i.e maximum charge drift time) t_a and maximum amplitude S_{aMAX} are found to be:

$$t_a = \frac{d_a R}{\mu_e V} \text{ and } S_{aMAX} = \frac{Ne}{2C_f}\frac{d_a}{R}, \qquad (2)$$

d_a being the track length normal to the anode.

However, when a uniform charge track of normal length d_s emanates from the *sample*, charge does not start disappearing linearly in time until the time t_s when the first electrons travel $R - d_s$ across the chamber to reach the anode. The resultant signal $S_s(t)$ is thus linear until t_s and then parabolic until t_R, the chamber's maximum transit time:

$$S_s(t) = \frac{Ne\mu_e V}{C_f R^2} t \ \textit{from } 0 \textit{ to } t_s, \text{ and} \qquad (3a)$$

$$S_s(t) = \frac{Ne\mu_e V}{C_f R^2}\left(t - \frac{(t - t_s)^2}{2(t_R - t_s)}\right) \textit{from } t_s \textit{ to } t_R, \qquad (3b)$$

where:

$$t_s = \frac{d_s R}{\mu_e V},\ t_R = \frac{R^2}{\mu_e V}, \text{ and } S_{sMAX} = \frac{Ne}{2C_f}\left(1 + \frac{d_s}{R}\right). \quad (4)$$

C. Distinguishing between points of emanation

From (2) and (4), the ratio of signal rise times between a track emanating from the anode and one emanating from the sample is simply d_a / R. Similarly, from (1) and (3), for anode and sample tracks of N_a and N_s electrons respectively, the signal amplitudes ratio as $N_a d_a / (N_s(R + d_s))$, where, depending upon angles of emission, d_a and d_s can each vary from zero to the maximum charge track length

We have therefore designed the detector chamber so that we can use both rise time and amplitude information to distinguish between alpha particle tracks that emanate from our sample and those that emanate from the detector's anode. This task is simplified by the fact that most alpha particle energies lie from 4-6 MeV and so the lengths L of their charge tracks also do not vary widely. In nitrogen these lengths are from 2.5 to 4.5 cm. Thus, for R of 15 cm (3 ×the maximum L) and V of 1000 V, sample risetime t_R equals 35 μs, while the maximum anode risetime t_a is only 35×4.5/15 = 10.5 μs, which is easily distinguished. Similarly, the maximum signal amplitude ratio is (taking N proportional to energy) (6×4.5)/(4×15) = 0.45 (about 2 to 1), which is also readily distinguishable.

With this understanding of how we hope to distinguish between anode and sample source events, it is clear that the detector chamber's sidewalls will present a problem, since an ionization tracks emitted from them can clearly generate risetime and signal amplitude values that will range between the limits set by the anode and sample signals. In our design the guard electrode is used to eliminate these signals. Any ionization tracks emanating from the sidewalls then induce charges in this guard electrode as they drift toward the anode plane and this signal is used to reject these events as invalid.

III. Representative Signal Traces

Figs. 1 – 5 show signal traces for five representative events. Fig. 1 shows the output traces from the anode and guard preamplifiers that result from an ionization track than emanates from the sample surface. The anode trace is large (about 930 ADC units) and has about a 30 μs risetime. The only guard signal is noise. Fig. 2 shows anode and guard traces from an ionization track that emanates from the anode surface. The anode trace is small (about 250 ADC units) and

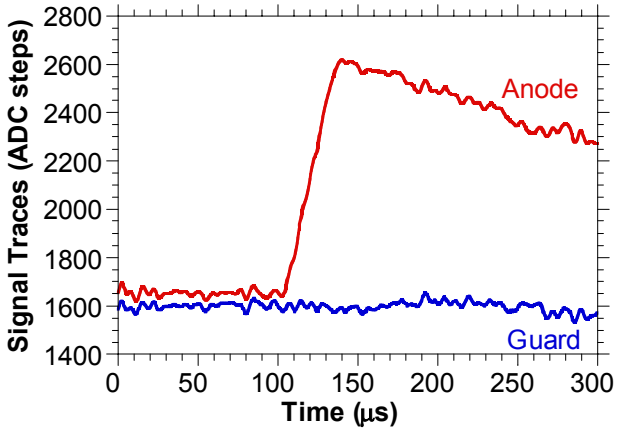

Fig. 1: Anode and guard traces; alpha particle emanating from the sample.

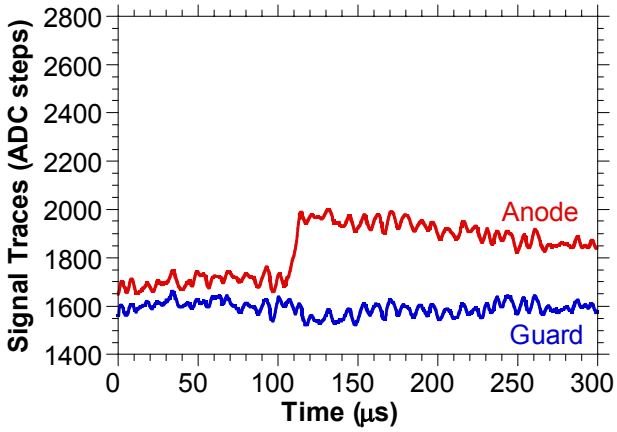

Fig. 2: Anode and guard traces; alpha particle emanating from the anode.

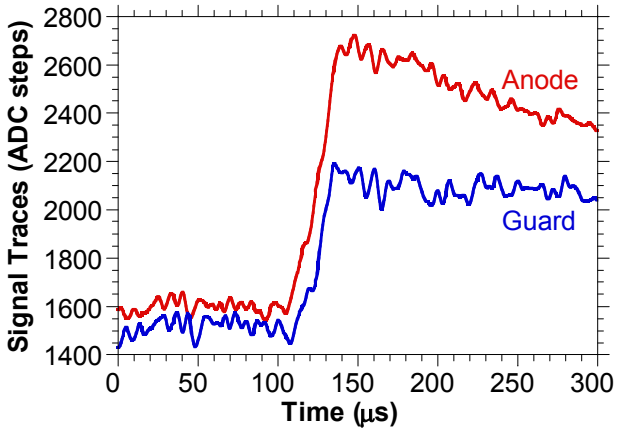

Fig. 3: Anode and guard traces; alpha particle emanating from close to the sample's edge.

has an 8 μs risetime. Again, there is no guard signal. Fig. 3 shows traces from an event whose ionization track lay partially under both the anode and guard electrodes. We know that it emanated from the edge of the sample both because the signals are large and because the risetimes are long. Fig. 4 shows traces from a event, where most of the charge was collected by the guard. The long risetimes tell us it emanated close to the sample, but it is not possible to tell whether it emanated from very close to the sample edge or from the sidewall. Because of this ambiguity, events of this type are always discarded, which reduces the counter's efficiency a bit, but guarantees its insensitivity to sidewall events. Fig. 5 shows a sidewall event with a nice example of induced charge effects. Its 30 μs risetime shows that it originated close to the sample. As the electrons initially drifted they moved closer to both the anode and guard electrodes and induced currents in both. However, as the majority approached the guard electrode and were finally collected onto it, they moved away from the anode, causing the induced current in the anode to reverse, leaving only a small amount of final charge on the anode. This happens quite rapidly as the electrons' field lines collapse onto the guard electrode and can no longer be described using the simple parallel plate model. We note that, in principle, a similar transient could be produced in the guard signal by a track lying entirely over the sample, but very close to its edge.

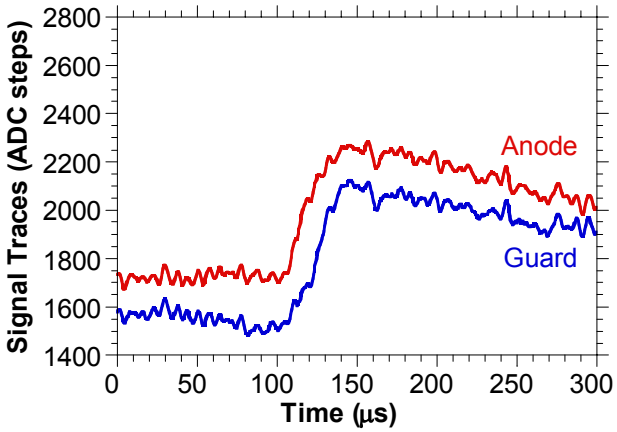

Fig. 4: Anode and guard traces; alpha particle emanating from the sidewall.

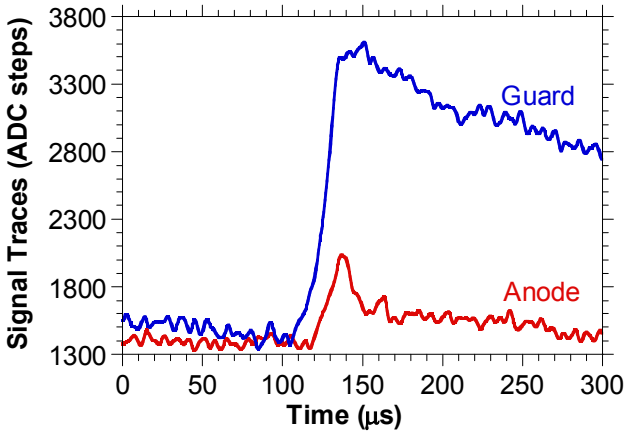

Fig. 5: Anode and guard traces; sidewall alpha particle's ionization track confined nearly entirely under the guard electrode.

IV. Pulse Shape Analysis Methods and Results

A. *Tests for Point of Emanation*

From the pulse shapes presented Sec. III, as well as from the theory of Sec. II, we have developed the following tests to determine if an ionization track emanated from the sample:

1) No guard signal: following any transients (i.e. the anode signal risetime is over) there should be no change in the guard signal's amplitude. This guarantees that the event's ionization track lies entirely beneath the anode electrode, which defines the area of the sample under test. These events could be either sample or anode emanating events.

2) Long risetime: our preferred method for distinguishing between sample and anode events. Risetimes greater than 25-30 μs come from sample events, while risetimes less than 10-15 μs come from anode events. Events with intermediate risetime values are generated by other mechanisms and contribute to the counter's background.

3) Amplitude: larger amplitudes are characteristic of sample side events. While not a definitive test, since many alpha particles will lose energy as they emanate from different distances below the sample surface and thus enter the counter with energies ranging, in principle, all the way to zero, a lower bound may be set to reliably remove anode side events.

B. The Trace Fitting Algorithm

We currently use an automatic fitting algorithm to measure pulse risetime and amplitude. The fitting function (See Fig. 6) consists three straight sections connected by two "hinges". The first and third sections are horizontal lines of length τ. Each section has two adjustable hinge parameters: its time location and its amplitude in ADC units (since the signals are captured directly as ADC output values). The section joining the hinges has no other adjustable parameters.

We find initial hinge parameters as follows. First the trace is differentiated and the times where it rises above and crosses below a preset threshold value are taken as the two hinge time parameters. Then, since the least squares fit to a horizontal line is the average function value over the line length, the trace averages over the two horizontal sections are chosen as the initial hinge ADC values. The variance between the trace and the fitting function is then computed as usual.

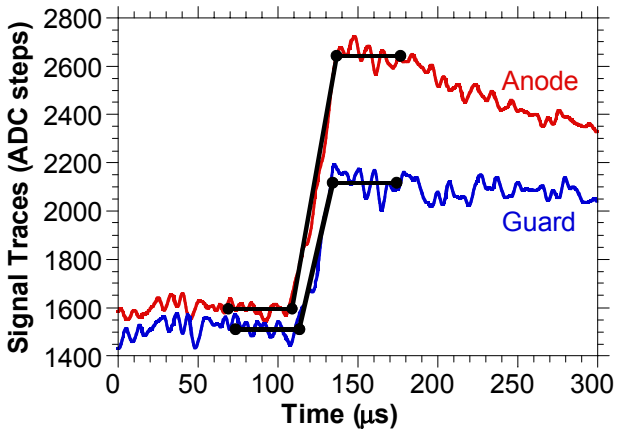

Fig. 6: The data of Fig. 3, showing the traces' pulse risetime fits..

Since our primary purpose in fitting the trace is to rapidly discriminate between sample and anode traces, our fitting routine is unusual in several regards. First, since our data arrive at 0.4 μs intervals, we only allow these intervals as hinge locations. Second, as we search in "hinge location space" for a best fit, we always compute the hinge amplitudes as the local average of the trace over their horizontal sections. Not having to optimize amplitudes based on the standard deviation of the entire function greatly speeds up the fit and has no significant effect on the risetime determination at the accuracy to which we require it. Third, since the number of points in the fitting function varies as the hinge locations are moved, we minimize the function $t^2 = \chi^2/(n-2))$, where n is the number of points in the fitting function and χ^2 is the variance between the trace and the fit. The minimization is carried out by selecting as set of sample times surrounding each initial hinge location (e.g. ±10) and then computing t^2 on the 2-dimensional grid of pairs hinge location values. The pair of hinge location values with the smallest value of t^2 then defines the best fit unless it lies on the edge of the grid, in which case the grid is expanded in that direction and the search repeated. Fig. 6 repeats Fig. 3, showing the resultant fits our method produces. Since both traces describe the same event with a single risetime, the difference between the fitted risetimes is therefore a measure of the error in our fits that arises from noise in the traces.

C. Fitting Results

Figs. 7-9 show data that we collected to explore our ability to discriminate between different points of alpha particle emanation. Three sets of data were taken using a thin 200 α/sec ^{230}Th source that was placed in the center of the sample area, in the center of the anode section, and in the center of a sidewall. Approximately 10,000 counts were collected for each source placement. The traces were then analyzed as described above, with the results shown in Fig. 7. As expected, the patterns associated with the three placements are quite different. The sample source pattern (blue) clusters for the most part above 30 μs risetime and 1000 ADC units, with a modest number of stragglers at lower amplitudes (α particle energies) as is appropriate for a thin source. The

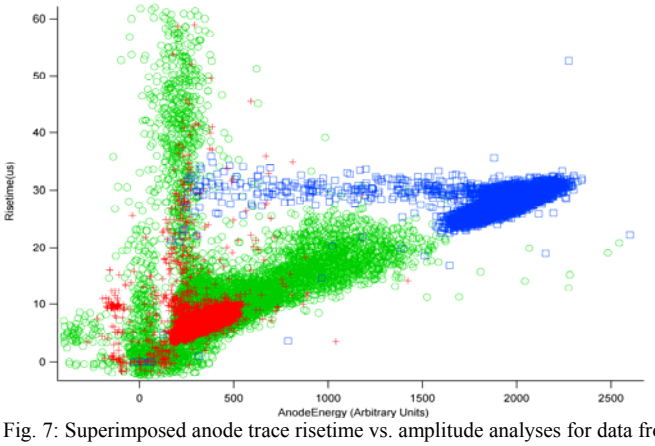

Fig. 7: Superimposed anode trace risetime vs. amplitude analyses for data from three source placements within the counter (sample, anode, & sidewall).

anode source pattern (red) clusters under 10 μs risetime and 250 ADC units. The dominant sidewall source pattern spans

the region between the other two patterns. Its branch going to quite large risetimes at amplitudes in the vicinity of 250 ADC units is of unknown origin. The branch at zero amplitude contains noise triggers. Fig. 7 clearly shows that if we were only to use the anode signal analysis, we would erroneously label a significant fraction of sidewall events as sample events.

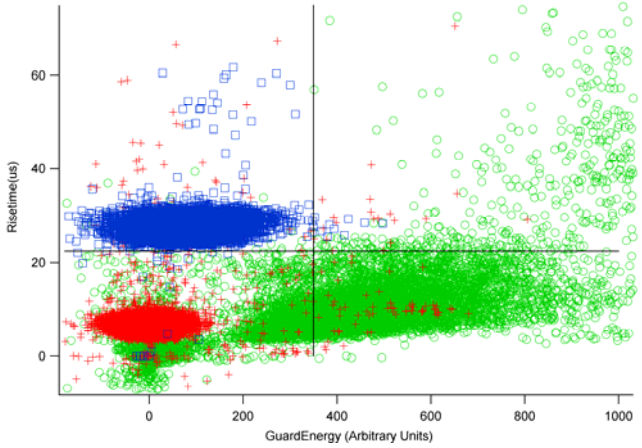

Fig. 8: Superimposed anode trace risetime vs. guard amplitude analyses for the same data as in Fig. 8.

Fig. 8 shows how we can effectively employ guard signal information by displaying anode signal risetime versus guard signal amplitude for the same three data sets. In this view the sidewall events clearly separate from both anode and sample events. We also note that both the anode and sample events show guard amplitudes that deviate significantly from zero in both positive and negative directions, with the sample set showing a larger spread. This spread is a measure of signal noise as fit by the fitting function. Since the risetimes of the sample signals are longer, their fits show larger random low frequency fluctuations and so a wider range of amplitude fits.

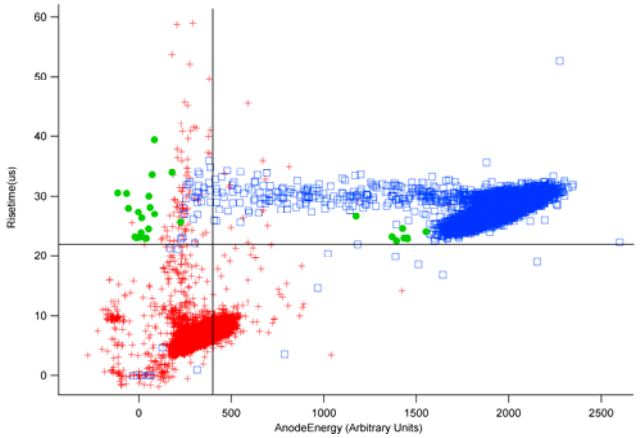

Fig. 9; The data of Fig. 7 after applying the guard energy and anode risetime cuts of Fig. 9 to the sidewall source data set.

Using the Fig. 8 view, we see that, by making the two cuts shown, at 22 μs for the anode risetime and XXX ADC units for the guard amplitude, we can easily exclude the majority of sidewall event. Fig. 9 show the data of Fig. 7 replotted after applying the cuts of Fig. 8 to the sidewall data set. We can now cut on anode amplitude to distinguish between anode and sample source events. The placement of this cut represents a tradeoff between efficiency (keeping as many low energy sample events as possible and specificity (rejecting as many anode events as possible). The shown anode cut is a good compromise as it misses only 25 out of 10,000 events (99.75% efficient) while accepting only 11 out of 10,000 anode events (0.11% anode fake rate). Further, only 7 out of 10,000 sidewall events are accepted (0.07% sidewall fake rate).

While it remains to be demonstrated that we can also achieve these low fake rates for alphas emanating from other locations within the counter, these results are very encouraging. For example, suppose we construct the counter from readily attainable "low alpha" materials (e.g. stainless steel and acrylic plastic) whose alpha emissivities are 0.01 α/cm^2-hr or less. Since our counter has about 2,600 cm^2 anode area and 3,050 cm^2 sidewall area, they will emit about 26 and 31 α/hr, each of which (by applying the fake rates) only 0.028 and 0.021 α/hr, will avoid our cuts and be accepted. Since the sample area is about 1,600 cm^2, this gives a counter background rate of only 0.00003 α/cm^2-hr. This rate is more than 100 times lower than the background rate of the best commercial instrument.

V. Conclusions

We have demonstrated a novel approach to measuring ultra-low alpha particle emissivities by adjusting the height of a N_2 filled ionization chamber so that pulse shape analysis may be applied to determining whether alpha particles emanate from the sample under test or from other parts of the counter. By rejecting the latter, we have shown that it should be feasible to measure samples having emissivities below 0.00005 α/cm^2-hr. Since this value exceeds the sensitivity required by semiconductor industry roadmaps for the coming decade by a factor of 10, and should also be useful in other applications as well, we have recently begun the development of a commercial instrument based on this technology.

VI. References

[1] R. Baumann and E. Smith, "Call for improved ultra-low background alpha-particle emission metrology for the semiconductor industry", *Int. SEMATECH Technology Transfer* #01054118A-XFR, 2001.

[2] The best commercially available instrument is the Model 1950 from Spectrum Sciences, Inc. Details are available from their website: www.ssi-iico.com.

[3] "Introduction to Charged-Particle Detectors" in *EG&G Ortec Catalog "Modular Pulse-Processing Electronics and Semiconductor Radiation Detectors"* p. 1.12 (97/98).

[4] W.K. Warburton, John Wahl, and Michael Momayezi, "Ultra-low background gas-filled alpha counter", *U.S. Patent 6,732,059* (Issued May 4, 2004).

[5] G. F. Knoll, *Radiation Detection and Measurement*, 3rd ed. New York, J. Wiley & Sons, 2000. Appendix D, pp. 789-794

[6] Knoll, Chapter 5.

[7] Y. Yorozu, M. Hirano, K. Oka, and Y. Tagawa, "Electron spectroscopy studies on magneto-optical media and plastic substrate interface," *IEEE Transl. J. Magn. Jpn.*, vol. 2, pp. 740-741, August 1987 [*Dig. 9th Annual Conf. Magn. Jpn.*, p. 301, 1982].

[8] M. Young, *The Technical Writer's Handbook.* Mill Valley, CA: University Science, 1989.